International Journal of Pharmaceutics 669 (2025) 125030

Contents lists available at ScienceDirect

International Journal of Pharmaceutics

journal homepage: www.elsevier.com/locate/ijpharm

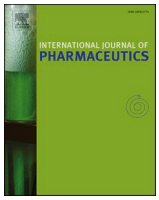

Effect of polyoxylglycerides-based excipients (Gelucire®) on ketoprofen amorphous solubility and crystallization from the supersaturated state

Serena Bertoni, Beatrice Albertini *, Nadia Passerini

Department of Pharmacy and Biotechnology, University of Bologna, Via S. Donato 19/2, 40127 Bologna, Italy

ARTICLE INFO

Keywords:
Poorly water-soluble drug
Supersaturation
Liquid-liquid phase separation
Crystallization inhibition
Oral bioavailability
Supersaturating formulations
Critical micelle concentration

ABSTRACT

Polyoxylglycerides-based solid mixtures, commercially known as Gelucire®, are excipients commonly used for bioavailability improvement of poorly water-soluble drugs. However, their effect on solutions containing hydrophobic drugs above crystalline solubility has not yet been explored. The goal of this study was to investigate the impact of a mix of two commercial Gelucire® with high HLB values (Gelucire®50/13 and Gelucire®48/16) on the amorphous solubility and crystallization from supersaturated solutions of ketoprofen, used as model drug. The results evidenced a strong interaction between Gelucire® components and the drug-rich nanodroplets generated upon liquid–liquid phase separation. This led to two important consequences: on one hand, the drug amorphous solubility was decreased, together with the amorphous-to-crystalline solubility ratio; on the other hand, the enlargement and coalescence of the drug-rich droplets were prevented. This stabilizing effect towards the drug-rich phase was comparable to, or even stronger than, that obtained with traditional amorphous polymers (PVP or HPMC) and contributed to inhibiting drug crystallization. Notably, the impact of Gelucire® on drug crystallization from the supersaturated state depended on its micellar behaviour: the monomeric form (below 50 μg/mL) accelerated the formation of crystals, whereas pre-micellar aggregates (50–500 μg/mL) and solubilizing micelles (above 500 μg/mL) inhibited drug crystallization. These findings will contribute to a better understanding of the behaviour of supersaturated drug solutions in the presence of Gelucire® and will facilitate the rational design of supersaturating drug delivery systems containing these excipients.

1. Introduction

Supersaturating drug delivery systems (SDDS) is an effective approach to improve the solubility and dissolution rate of poorly water-soluble compounds. These formulations are able to generate drug supersaturation after dispersion or dissolution in gastrointestinal fluids and maintain it for a physiologically relevant time, thus representing a boost for drug absorption. In SDDS, the drug can be either in solution (e.g., cosolvent systems, lipid-based formulations) or in a high-energy solid form (e.g., amorphous forms, crystalline salt forms, co-crystals and amorphous solid dispersions (ASD) like) (Brouwers et al., 2009). In both cases, supersaturation is achieved when drug molecules are dissolved at a concentration above the equilibrium crystalline solubility (Dahan et al., 2016).

It has been shown that highly supersaturated solutions undergo phase separation when the amorphous solubility of the drug is exceeded, with formation of drug rich-droplets dispersed within the aqueous phase. This phenomenon is known as liquid–liquid phase separation (LLPS) and it has been extensively studied by the research group of Taylor and co-workers (Ilevbare and Taylor, 2013; Raina et al., 2015). When a supersaturated solution undergoes LLPS, a metastable equilibrium takes place between free drug in the bulk aqueous solution and the non-crystalline, water-saturated, drug-rich phase (Miao et al., 2019). The interest in studying this phenomenon arises from the recognition of its role as "drug reservoir" maintaining the maximum drug concentration in the bulk solution while the permeation through the intestinal membrane occurs. However, the dispersed drug-rich phase is thermodynamically unstable, and thus there is a constant driving force toward crystallization to lower the system's free energy by reducing the concentration of free drug (Indulkar et al., 2020). When crystallization occurs, nucleation followed by crystal growth rapidly depletes drug supersaturation up to a drug concentration that approaches the crystalline equilibrium solubility.

Various studies have shown that excipients might affect both the maximum supersaturation (amorphous solubility) and the crystallization tendency from supersaturated solution. The role of polymers as

* Corresponding author.
E-mail address: beatrice.albertini@unibo.it (B. Albertini).

https://doi.org/10.1016/j.ijpharm.2024.125030
Received 22 August 2024; Received in revised form 2 December 2024; Accepted 2 December 2024
Available online 5 December 2024

crystallization inhibitors is well studied. Some polymers are able to delay or inhibit drug crystallization either from solution or in a solid matrix. They can impact either nucleation by interacting with the drug aggregates that form crystal nuclei, or growth by being adsorbed onto the developing crystal surfaces (Indulkar et al., 2020). In addition to polymers, surface active materials might also impact the crystallization processes by influencing nucleation and crystal growth (Dai et al., 2008; Chen et al., 2015) or accelerating solution-mediated polymorph transformation (Semjonova and Bērziņš, 2022). However, the mechanisms underlying these effects are still poorly understood. Furthermore, the amount of amphiphilic excipients (whether above or below the critical micelle concentration, CMC) is a determining factor, as the monomeric and micellar forms can interact differently with the drug-rich droplets and the crystal nuclei in supersaturated drug solutions (Indulkar et al., 2020).

Polyoxylglycerides-based solid mixtures, commercially known as Gelucire® with high Hydrophylic Lipophylic Balance (HLB), are a widespread class of excipients for developing self-emulsifying and/or supersaturating drug delivery systems aimed at improving the bioavailability of poorly water soluble drugs (Bertoni et al., 2020; Bertoni et al., 2019; Qi et al., 2010). These semicrystalline carriers, classified as GRAS, are composed of polyethylene glycol (PEG) esters of long chain fatty acids, mono-, di- and triglycerides (Panigrahi et al., 2018). They have low melting temperatures and are thus suitable to be processed by solvent-free manufacturing technologies such as hot melt extrusion (Uttreja et al., 2024), melt granulation (Sarabu et al., 2021), spray congealing (Bertoni et al., 2019; Qi et al., 2010) and 3D printing (Daravath, 2021; Vithani et al., 2019). They have been used either alone (Aldosari et al., 2021) or in combination with polymers, oils and surfactants to produce different types of dosage forms (Shin et al., 2019; Goo et al., 2021). Due to their amphiphilic character, Gelucire® excipients with high HLB have excellent solubilizing properties and have proved to be efficient bioavailability enhancers for drugs. A number of studies have demonstrated their effectiveness in the development of formulations with improved performance in terms of *in vitro* solubility and dissolution rate (Bertoni et al., 2020; Sarabu et al., 2021; Albertini et al., 2015), as well as *in vivo* oral bioavailability (Bertoni et al., 2019; Aldosari et al., 2021; Shin et al., 2019).

Despite the interest in using these excipients, their effect on solutions containing hydrophobic drugs above crystalline solubility has not yet been explored. The goal of this study was to investigate the influence of high-HLB Gelucire® on supersaturated solutions of poorly water-soluble drugs. Specifically, two commercial Gelucire® excipients with high HLB values (Gelucire®50/13 and Gelucire®48/16) mixed at 1:1 wt ratio (hereinafter referred to as Gel-mix) were used and evaluated regarding their influence on:

(i) the drug crystalline solubility (i.e., solubilization in the aqueous bulk phase);
(ii) the drug amorphous solubility (i.e., LLPS onset);
(iii) the properties of the colloidal drug-rich phase formed when amorphous solubility is exceeded;
(iv) drug crystallization from supersaturated solutions.

Ketoprofen (KET), which belongs to class II of the BCS, was selected as model drug. First, KET crystalline and amorphous solubility were determined in the presence of several Gel-mix concentrations. The impact of Gelucire® excipients on the properties of the KET-rich colloidal phase formed at concentrations above the amorphous solubility was investigated. In parallel, the influence of Gelucire® on KET crystallization from supersaturated solutions was evaluated.

2. Materials

Ketoprofen (KET) was purchased from Merck (Darmstadt, Germany). Gelucire®50/13 and Gelucire®48/16 were kindly supplied from Gattefossè (Milan, Italy). Methocel E5 (HPMC) was a gift of Colorcon and PVP K-30 (Kollidon®30) was kindly supplied by BASF S.p.A. (Ludwigshafen, Germany). In order to have the drug molecule in non-ionised form, the aqueous medium used for all experiments was NaCl/HCl buffer (0.2 M, pH 1.2). All other chemicals and solvents used were of analytical grade.

3. Methods

3.1. Determination of critical micelle concentration (CMC) of Gelucire

The CMC of Gel-mix was evaluated in NaCl/HCl buffer (0.2 M, pH 1.2) at concentrations ranging from 1 to 2000 μg/ml. The solutions were prepared by dilution of a stock solution containing 2.0 mg/ml of Gel-mix with the same buffer, and analysed using different techniques:

Surface tension measurement: Surface tension analysis was performed by a tensiometer (Kruss tensiometer K8600, Hamburg, Germany) with the Du Noüy ring method. First, the accuracy of the platinum-iridium ring was validated by determining the surface tension of water (72 ± 0.3 mN/m). Then, 4 ml of Gelucire solutions were transferred in a glass vessel which was thermostated at 37 °C by a water bath and the surface tension was measured. Measurements were repeated six times for each sample and the mean ± SD was calculated. The CMC was determined from a plot of the surface tension values versus Gel-mix concentration.

Turbidity measurement by UV spectroscopy: Absorption spectra of samples were taken using Cary 60 UV–Visible spectrometer (Agilent Technologies GmbH, Waldbronn, Germany) at 350 nm. The absorption spectra of samples were acquired using Quartz sample cells with optical paths of 10 mm after correction with solvent spectra. A plot of the turbidity of the solution at increasing surfactant concentration is generally characterized by a low slope for dilute solutions and a steeper one for solutions above the CMC. Thus, the CMC was determined from a plot of the absorbance as a function of Gel-mix concentration.

Light scattering: Light scattering technique is well suited for the determination of the CMC. Below the CMC, the intensity of scattered light detected is similar to that obtained in simple buffer. However, once the CMC is reached, the intensity of scattered light increases due to the presence of micelles. A Brookhaven 90-PLUS instrument (Brookhaven Instruments Corp., Holtsville, NY, USA) with an He-Ne laser beam at a wavelength of 532 nm (scattering angle of 90°) was used for measurements of Gelucire solutions. Both a plot of the intensity of scattered light (in million counts per second) and micelle size (in nanometers) as a function of Gel-mix concentration were obtained.

Ketoprofen crystalline solubility. The equilibrium (crystalline) solubility of KET (S_{eq}) was determined by shake-flask method, adding an excess amount of crystalline KET to 5 ml of NaCl/HCl buffer (0.2 M, pH 1.2) and in solutions of Gel-mix at concentrations ranging from 1 to 2000 μg/ml pre-dissolved in the same buffer. The solutions were agitated for 48 h at 37 °C. The samples were centrifuged at 14000 rpm, the supernatant was diluted and analysed by high performance liquid chromatography (HPLC). The HPLC system consisted of two mobile phase delivery pumps (LC-10ADvp, Shimadzu, Japan), a UV–Visible detector (SPD-10Avp, Shimadzu, Japan), and an autosampler (SIL-20 A, Shimadzu, Japan). A Luna C18 column (150 mm × 4.60 mm, 5 μm) was used with a mobile phase consisting of 50 % of water acidified with 0.1 % trifluoroacetic acid and 50 % of acetonitrile. The injection volume was 20 μl, the flow rate was 1 mL/min, and the detection wavelength were set at 259 nm. Standards (1–50 μg/ml) were prepared by diluting with mobile phase a KET stock solution prepared in acetonitrile, exhibited good linearity ($r^2 = 0.9962$) over the concentration range. Moreover, to compare the effect of Gelucire with commonly used hydrophilic polymers, the solubility in solutions containing polymers (PVP and HPMC, 100 μg/ml and 1000 μg/ml) was also determined.

Ketoprofen amorphous solubility. The amorphous solubility (S_{am}) of KET was determined by the UV-extinction method. A concentrated solution of KET (50 mg/ml) was prepared by solubilizing the drug in

DMSO. This solution was gradually added (50 μL/min) to 250 ml of aqueous buffer kept at 37 °C with a magnetic stir bar at 300 rpm, in order to generate a supersaturated solution. The final DMSO content was less than 1.2 % (v/v). Supersaturated solutions were monitored for changes in scattering using a UV/vis spectrophotometer at non-absorbing wavelength (350 nm) using a Cary 60 UV–Vis spectrometer (Agilent Technologies GmbH, Waldbronn, Germany). The formation of a second phase, i.e., LLPS, caused an increase in scattering that can be detected by an increase in the extinction between 280–450 nm. The concentration at which a sharp increase in scattering was observed corresponded to the LLPS onset and to the amorphous solubility of the drug. The amorphous solubility of KET was determined in NaCl/HCl buffer (0.2 M, pH 1.2), in solutions of Gel-mix at concentrations ranging from 1 to 2000 μg/ml pre-dissolved in the same buffer, and in solutions of polymers (PVP and HPMC, 100 μg/ml) in the same buffer.

Analysis of the size and polydispersity of the colloidal drug-rich phase. Aliquots of a concentrated stock solution of KET (50 mg/ml, DMSO) was added to the buffer, Gel-mix and polymer solutions under stirring at 250 rpm. The resulted solutions were prepared to have a final KET concentration either below (Sa – 100) or above (Sa + 50, Sa + 100, Sa + 150) to the amorphous solubility value. The final DMSO concentration in these solutions was equal or less than 1.2 % (v/v). The temperature was maintained at 37 °C during sample preparation. The particle size and polydispersity index (PDI) of the KET-rich droplets generated upon LLPS were evaluated by photon correlation spectroscopy (PCS) using a Brookhaven 90-PLUS instrument (Brookhaven Instruments Corp., Holtsville, NY, USA) with an He-Ne laser beam at a wavelength of 532 nm (scattering angle of 90°).

Crystallization experiments KET concentrated stock solution (50 mg/ml DMSO) was added to 10 ml Gel-mix solutions ranging from 1 to 2000 μg/ml to achieve a concentration equal to the amorphous solubility. Solutions were kept at 37 °C and 300 rpm agitation. The time at which solutions turned cloudy with presence of solid particles was taken as crystallization time. The size of KET crystals was determined by optical microscopy using a Nikon Eclipse E400 optical microscope connected to a Nikon Digital Net Camera DN100 for the image acquisition. Then, dried KET crystals were obtained by filtration of supersaturated KET solutions in buffer pH 1.2, washed with the same solvent and drying overnight. Samples of 4–6 mg were analyzed by differential scanning calorimetry (DSC) using a Perkin Elmer DSC 6. DSC experiments were performed in a dry nitrogen atmosphere (20 ml/min), heating the samples at a rate of 10 °C/min from ambient temperature to 150 °C.

4. Results

4.1. Gelucire micellar behaviour in solution

Aggregation of surface-active agents occurs at a critical concentration, which is referred to as critical micelle concentration (CMC). This point can be measured experimentally as it corresponds to a variation of one physical properties of the system (e.g. surface tension, conductivity or turbidity) (Miller et al., 2001; Perinelli et al., 2020). Due to their amphiphilic nature, the behaviour of high HLB Gelucire® excipients following dilution in aqueous medium should exhibit similar self-aggregation properties in order to lower the free energy of the system. The micellar behaviour of Gel-mix was investigated by three different methods.

The measured surface tension *vs* concentration plot is shown in

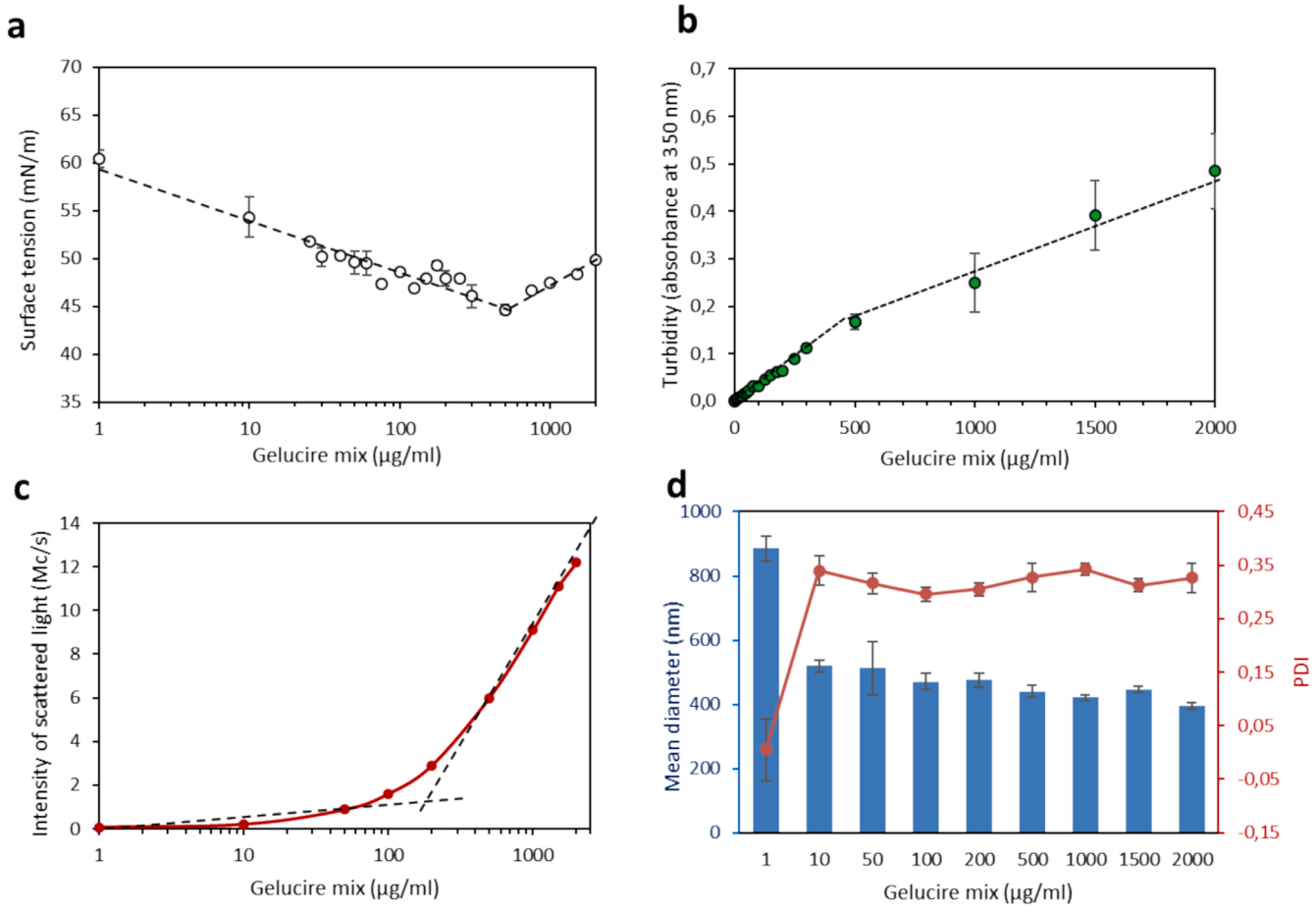

Fig. 1. (a) Surface tension measurement of Gel-mix solutions; **(b)** turbidity (scattering) of Gel-mix solutions; **(c)** intensity of scattered light (in million counts per second) and **(d)** particle diameter and PDI of Gel-mix solutions.

Fig. 1**a**. The surface tension of pure acidic buffer solution at 37 °C was 64.3 ± 1.2 mN/m. The surface tension decreased with increasing Gel-mix amount, reaching a minimum at 500 μg/ml and above this concentration value the surface tension showed a slight increment. Another physical parameter affected by the micellization of surfactants is the turbidity of the solution. Fig. 1**b** showed that the turbidity intensified with increasing Gel-mix concentrations, as showed by the increase in the light scattered at 350 nm. A change in the slope of the scattering values was observed at Gel-mix concentration of 500 μg/ml, above which the turbidity increases at a lower rate. Finally, the formation of micelles was confirmed by the detection of colloidal species by DLS (Fig. 1**c** and Fig. 1**d**). Starting from a concentration of 10 μg/ml, aggregates with size of about 500 nm were observed. The intensity of the scattered light, expressed as count rate per seconds (Fig. 1c), which is proportional to the number of micelles formed in solution, increased slowly from 10 to 500 μg/ml, while a steeper increase was noted above 500 μg/ml. The maximum increase in the number of colloidal particles detected, in fact, was at a concentration range between 500 and 1000 μg/ml (Fig. 1c) although the first colloidal aggregates were detected starting from 10 μg/ml. Gelucire® micelles had size between 400 and 500 nm and PDI between 0.300 and 0.350. Specifically, the diameters slightly decreased with increasing Gel-mix concentration and at 500 μg/ml, the colloidal system presented size of 440 nm and PDI of 0.327 (Fig. 1d).

4.2. Determination of KET crystalline and amorphous solubility

The solubility of crystalline KET (S_{eq}) in pH 1.2 buffer was found to be 161 ± 5 μg/ml, in accordance to a previously reported value of 0.13 mg/ml measured at 37 °C in a similar acidic medium (Yazdanian et al., 2004). The values of KET S_{eq} in presence of increasing Gel-mix amounts are reported in Fig. 2. In presence of low concentrations of pre-dissolved Gel-mix (1–750 μg/ml), KET solubility showed small variations, as shown by the mild slope (Fig. 2). However, a substantial increase in the drug equilibrium solubility was observed starting from Gel-mix concentration of 750 μg/ml. With 2000 μg/ml of Gel-mix, the KET equilibrium solubility was enhanced up to 410 μg/ml, i.e., more than 2.5 times compared to simple buffer.

As regards amorphous solubility, dissolution of amorphous solid was initially performed by dissolving a film of amorphous KET obtained by rapid cooling of molten KET. Unfortunately, crystallization during experiment on the surface of the amorphous solid was observed prior to attainment of LLPS, impeding the determination of the amorphous solubility. Therefore, another approach was adopted. The amorphous phase was generated by creating a supersaturated solution adding a concentrated drug solution in an organic solvent to the buffer of interest and the UV extinction method was used to monitor the real-time scattering intensity changes at a non-absorbing wavelength. The specific experimental setup adopted is shown in Fig. 3**a**. A similar approach has been used to determine the amorphous solubility and LLPS of numerous hydrophobic compounds (Ilevbare and Taylor, 2013; Nguyen et al., 2023; Wang et al., 2023). The extinction plot obtained is shown in Fig. 3**b**: the continuous addition of KET concentrated solution to acidic buffer led to supersaturated solutions. In the region between the crystalline and amorphous solubility, the solution is a one phase supersaturated solution. At a certain point, the solutions turned cloudy with a slight bluish color and an increase in scattering was detected, indicating the formation of a second liquid phase i.e., LLPS. This value was taken as KET amorphous solubility (S_{am}). In simple buffer, LLPS occurred at a KET concentration of 453.0 μg/ml. Following LLPS, however, the turbidity of the solutions only lasted few minutes, gradually disappearing with rapid formation of small solid particles of crystallized KET. However, it was possible to detect LLPS prior to drug crystallization in all experiments (repeated at least in triplicate). The S_{am} of KET was determined in simple buffer and in presence of increasing Gel-mix concentration. As observed in Fig. 3**c**, the presence of Gel-mix had a profound influence on KET LLPS onset. Moreover, drug crystallization was detected during UV-extinction experiments only with certain Gel-mix concentrations. Table 1 shows the effect of Gel-mix on the time at which KET crystallized after LLPS, taking as zero the LLPS onset and with continuous KET additions (see Methods, determination of KET amorphous solubility). The data show a significant crystallization inhibition effect starting from 50 μg/ml of Gel-mix.

Fig. 4**a** shows the calculated values of KET S_{am} at increasing Gel-mix concentration, compared with the corresponding S_{eq} values. Then, the ratio of the amorphous solubility and the crystalline solubility (LLPS/equilibrium solubility), corresponding to the maximum supersaturation achieved when phase separation occurred, was calculated (Fig. 4**b**). Observing the evolution of S_{eq} and S_{am} in Fig. 4a, three regions can be identified:

(i) with low Gel-mix amount (0–50 μg/ml), the crystalline solubility was not significantly enhanced. In contrast, the amorphous solubility decreased from 453 μg/ml in simple buffer to values around 300 μg/ml;

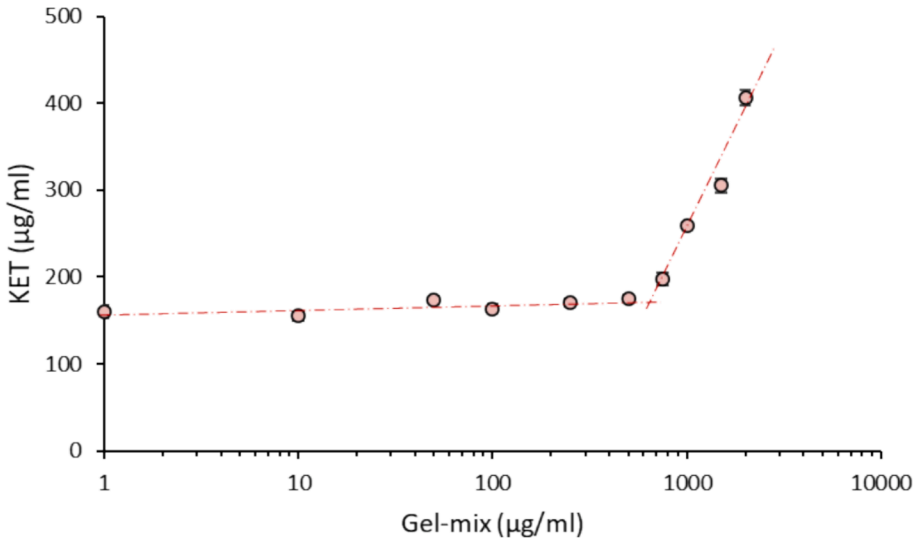

Fig. 2. Crystalline equilibrium solubility (S_{eq}) of KET in solutions of Gel-mix at increasing concentration in buffer pH 1.2.

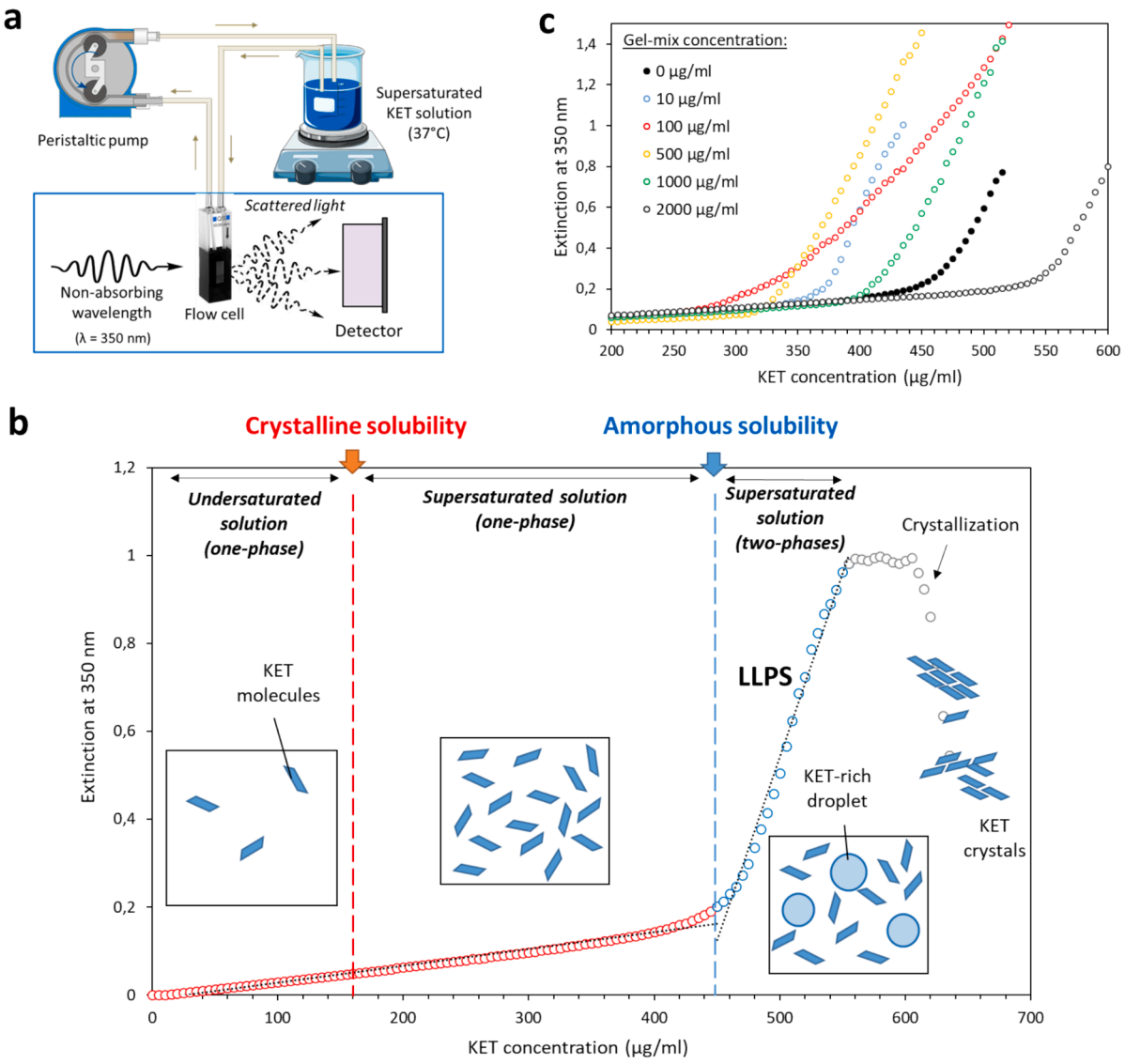

Fig. 3. **(a)** schematic representation of the experimental setup used for determination of amorphous solubility: the supersaturated drug solution is continuously pumped into a quartz flow-through cell and the real-time scattering intensity changes at a non-absorbing wavelength (350 nm); **(b)** schematic representation of the UV Extinction plot at increasing KET concentration in buffer pH 1.2; **(c)** extinction measurement obtained in presence of various Gel-mix concentration. For clarity, only the extinction values following a linear trend (i.e. before KET crystallization) are shown.

Table 1
Evaluation of KET crystallization in solutions exhibiting LLPS at increasing Gel-mix concentration. In case of observed crystallization, the time needed for KET crystallization after LLPs onset (min) is reported.

Gel-mix concentration (µg/ml)	Crystallization during UV-extinction experiment	Crystallization time after LLPS onset
0	yes	8.5 ± 1.8
1	yes	8.0 ± 0.1
10	yes	7.7 ± 0.2
50	yes	10.9 ± 1.8
100	yes	26.1 ± 1.4
250	yes	26.2 ± 1.3
500	yes	25.3 ± 1.7
750	no	> 30
1000	no	> 30
1500	no	> 30
2000	no	> 30

(ii) with Gel-mix amounts between 50 and 250 µg/ml, both the crystalline and the amorphous solubility remained constant with average values of 170 and 300 µg/ml, respectively;
(iii) with Gel-mix concentrations above 500 µg/ml, both crystalline and amorphous solubility gradually increased with higher Gelucire amounts.

The amorphous-to-crystalline solubility ratio (Fig. 4b) of KET decreased from 2.8 in simple buffer, up to a constant value of about 1.5 in presence of Gel-mix at concentration of 50 µg/ml. Above this value, the amorphous-to-crystalline solubility ratio of KET remains unchanged.

Then, the effect of Gel-mix of KET S_{eq} and S_{am} was compared with those of two polymeric excipients commonly used in SDDS, polyvinylpyrrolidone (PVP) and hydroxypropylmethylcellulose (HPMC), all pre-dissolved in the buffer at two concentrations, one below (100 µg/ml) and one above (1000 µg/ml) Gel-mix CMC value. (Fig. 4**c**). The results evidenced a similar trend for the three excipients used at 100 µg/ml. While the S_{eq} of KET was slightly enhanced from 161 µg/ml to 170–200 µg/ml, all excipients had a negative impact on S_{am}, causing a decrease of the maximum drug concentration achievable in supersaturated solution.

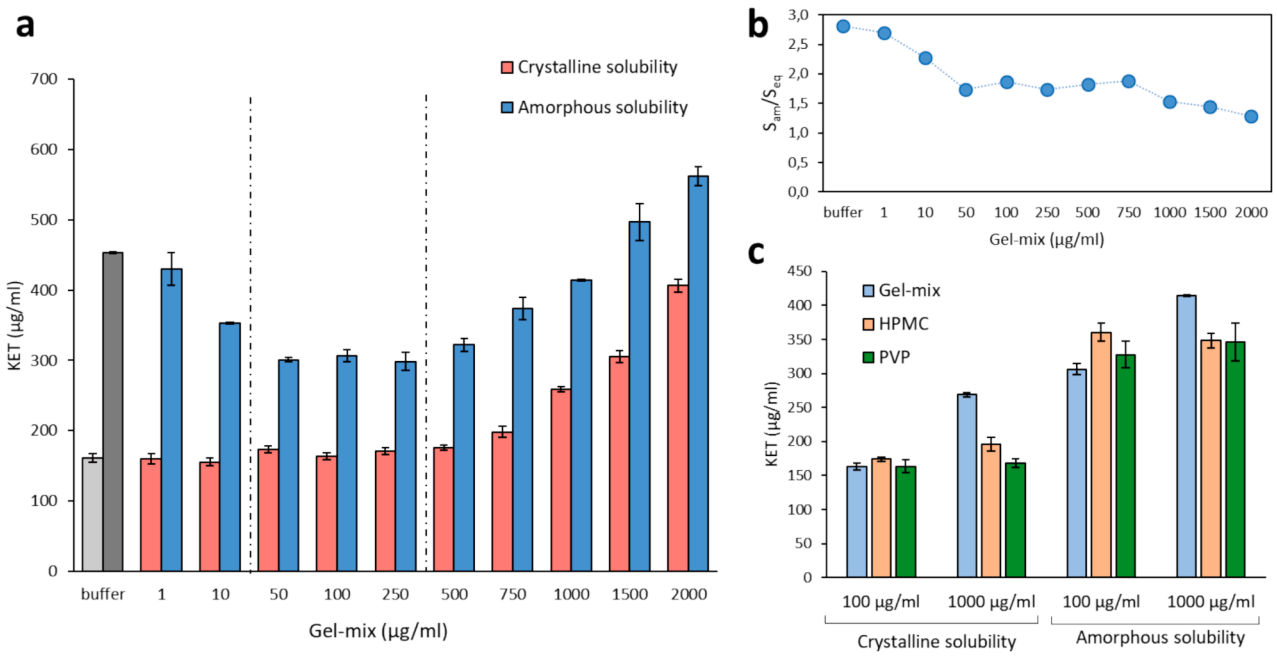

Fig. 4. **(a)** Effect of Gel-mix on the solubility of KET. Summary of experimental data of KET crystalline (S_{eq}) and amorphous (S_{am}) solubility; **(b)** measured KET amorphous-to-crystalline solubility ratio and **(c)** effect of Gel-mix compared to PVP and HPMC at 100 µg/ml and 1000 µg/ml on KET crystalline (S_{eq}) and amorphous (S_{am}) solubility.

A different behaviour was observed with excipients concentrations of 1000 µg/ml: both the S_{eq} and the S_{am} of KET were higher in Gel-mix solution compared to solutions of PVP or HPMC at equal concentrations.

4.3. Effect of Gelucire on the KET-rich nanodroplets

Fig. 5 shows the size and PDI of freshly prepared KET-rich droplets in solutions at three supersaturation levels (50, 100 and 150 µg/ml above S_{am}) in simple buffer and with Gel-mix, PVP or HPMC. In simple buffer, the droplets had an initial size of about 650 nm. With increasing KET concentration, the droplets became bigger (around 900 nm) approaching the micron size. Differently, the presence of Gel-mix at 100 µg/ml led to the formation of drug-rich droplets with size below 200 nm and PDI between 0.20 and 0.24. Further KET amounts did not cause an increase in droplet size, which remained in the range 170–190 nm. In HPMC solution, KET droplets showed diameters of approximately 216 nm, increasing to 260 nm at the highest KET concentration (S_{am} + 150). Differently, the presence of PVP could not inhibit the droplets enlargement and KET nanodroplets exhibit a gradual increase in diameter passing from 370 nm to 455 nm and further exceeding 530 nm.

4.4. Effect of Gelucire on KET crystallization from supersaturated solutions

The influence of Gelucire on KET crystallization from supersaturated solutions at equal supersaturation levels (concentration approaching its S_{am}) was assessed and the crystallization time and morphology of KET crystals are shown in Fig. 6**a** and Fig. 6**b**, respectively. In the absence of any additive, KET crystallizes after 64 min in large plate-like crystals with dimensions up to 50 µm. Low amounts of Gel-mix promoted crystallization of KET, as the crystallization times was reduced to 20 and 13 min with 1 and 10 µg/ml of Gel-mix, respectively. Higher additive

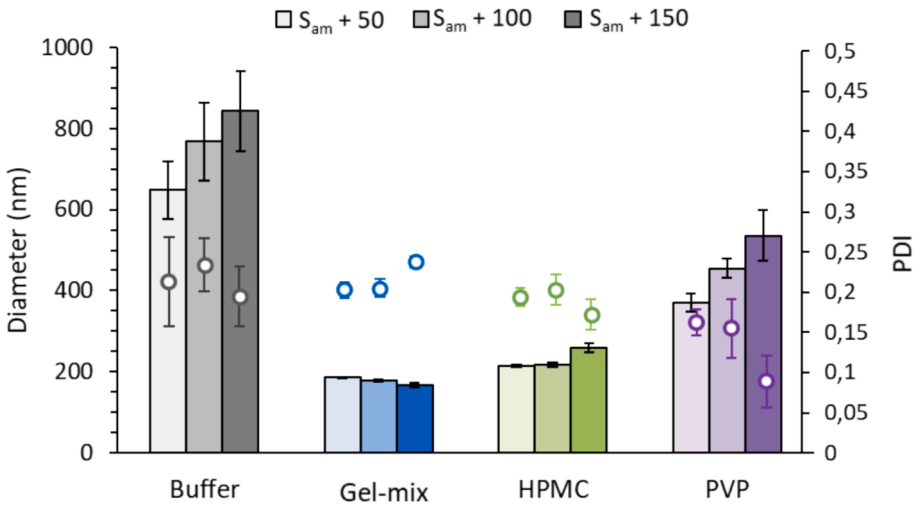

Fig. 5. Particle Size and polydispersity index (PDI) of KET-Rich Droplets at 37 °C in presence of Gel-mix, PVP and HPMC at 100 µg/ml. Diameter size are indicated by bars and PDI values by circles.

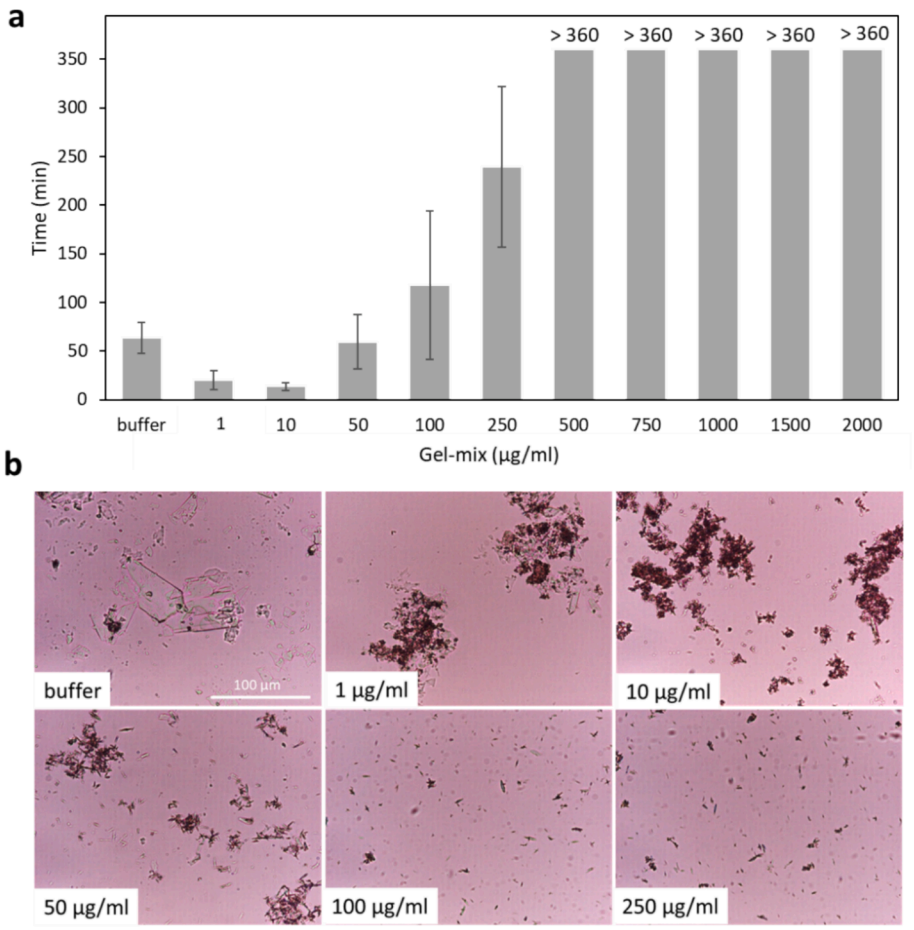

Fig. 6. **(a)** Crystallization time from KET supersaturated solutions in buffer pH 1.2 and with increasing Gel-mix concentrations at KET concentrations equal to S_{am} and **(b)** optical microscopy images of KET crystals obtained after crystallization from supersaturated solutions.

concentrations determined an inverse trend on drug crystallization time. Starting from Gel-mix concentrations of 10 µg/ml, the highest the Gel-mix amount, the longest the time of inhibition of drug crystallization. Above 500 µg/ml, the crystallization was delayed for more than 360 min. This crystallization inhibition effect of Gelucire micelles reflected also in the morphology of the resulting crystals, which were characterized by needle-like crystals with size smaller than 5 µm.

KET crystals were analysed by DSC and results are shown in Fig. 7. DSC curves shows that all samples crystallized in Gelucire solutions present lower melting temperature (T_m) compared to crystals obtained in buffer, having a T_m of 96 °C. Specifically, a distinction can be observed between samples crystallized in Gelucire solutions in the pre-micellar region (up to 500 µg/ml) and those crystallized in Gelucire solutions above CMC. The former crystals exhibit an important melting point depression (T_m of about 90 °C), while the T_m of the latter crystals was depressed to a lower extent (T_m of about 93 °C) and a second endothermic event at 58 °C related to Gel-mix was detected.

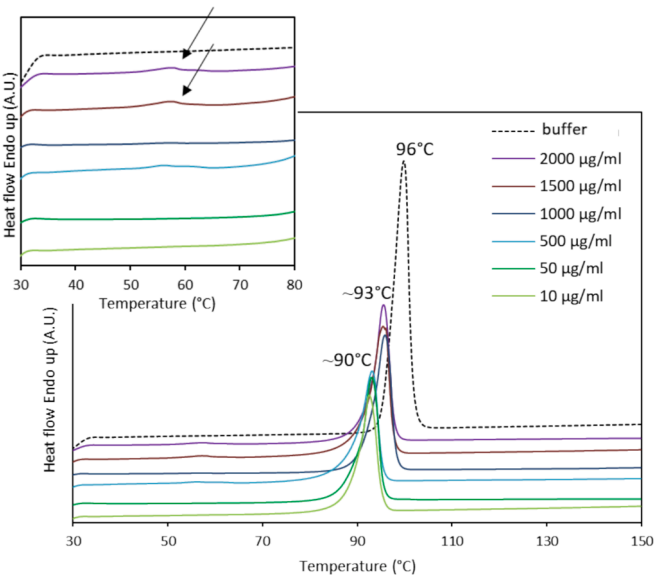

Fig. 7. Thermograms of the KET crystals obtained upon crystallization from supersaturated solutions (KET concentration equal to S_{am}) with increasing Gel-mix concentrations; the inset plot shows an enlargement of the curves between 30 and 80 °C.

5. Discussion

5.1. Oral bioavailability of supersaturating dosage forms: Impact of supersaturation and solubilization

For many enabling SDDS formulations, a combination of supersaturation and solubilization occurs. A supersaturated solution is generated when the activity of the dissolved drug in solution exceeds the activity of the drug in the saturated solution of the thermodynamically stable form (Mullin and Söhnel, 1977). Clearly, both the extent and the duration of the supersaturation state in the gastrointestinal lumen are crucial to

determine the improved solubility and absorption by SDDS (Alhayali et al., 2018). The excipients of the formulation, such as polymers and surfactants, can solubilize during dissolution and once in solutions can interfere with the drug phase behaviour. Specifically, they can positively or negatively influence the maximum achievable drug supersaturation and the drug crystallization from the supersaturated state. Thus, the impact of excipients commonly found in SDDS on these aspects must be considered in order to achieve a successful formulation in terms of extent and duration of supersaturation.

In the development of SDDS, beside supersaturation, also the process of solubilization should be considered. Drug solubilization may depend on the presence of surface active or solubilizing additives added to the formulation, as well as on the effect of endogenous amphiphiles involved in the digestion process in the GI tract (e.g., phospholipids and bile salts). The solubilization process of the drug by amphiphilic compounds leads to an increase in the total amount of drug in solution i.e., apparent solubility, as a result of the extra amount of drug that can be solubilized into micelles. However, this process does not modify the solute activity, which depends on the amount of "free" drug in solution. The difference between supersaturation and solubilization acquires a clear relevance when considering that only the amount of "free" drug in solution determines the solute flux through membrane (Raina et al., 2015) and, therefore, have an impact on the solubility advantage achieved by SDDS.

5.2. Solubilizing effect of Gelucire

Gelucire® excipients with high HLB are reported to be able to self-emulsify in contact with aqueous media forming a fine dispersion (Zoubari et al., 2017). Changes in the surface tension, turbidity and scattered light of Gel-mix solutions confirmed that these materials are able to form a micellar dispersion in aqueous media. The micellization process was observed to happen at a concentration range rather than a single value corresponding to the CMC. This can be explained by the heterogeneous composition of Gelucire®, which consist in highly hydrophobic components (di- and tri-glycerides), small-sized amphiphilic moieties with hydrophobic character (monoglycerides), amphiphilic components with large hydrophilic head group (PEG esters of fatty acids) and finally some free PEG which is likely to assemble in the outer micellar layer. A simplified scheme of the micellar aggregation of Gelucire® moieties is represented in Fig. 8. Unlike single-molecule surfactants (e.g., sodium dodecyl sulfate), surfactant mixtures exhibit a much more complex micellar behavior (Reporting Experimental Data Dealing with Critical Micellization Concentrations c.m.cR8S2Q1M7s of Aqueous Surfactant, 1979). In these cases, the 'transition range' can broaden, as the composition of the micelles varies with the total concentration (Reporting Experimental Data Dealing with Critical Micellization Concentrations c.m.cR8S2Q1M7s of Aqueous Surfactant, 1979).

This behaviour is consistent with the gradual changes in the physical properties of solutions with increasing Gel-mix concentrations, where the middle points (corresponding to the sharpest changes) observed were approximately at 500 μg/mL. The reported CMC values of the individual excipients (which are themselves composed of a mixture of components) Gelucire®50/13 and Gelucire®48/16 are 100 mg/L and 153 mg/L (25 °C), respectively (Gattefossè website. https://www.gattefosse.com/pharmaceuticals/product-finder/gelucire-4816 (accessed 18 July, 2024; Gattefossè website. https://www.gattefosse.com/pharmaceuticals/product-finder/gelucire-5013 (accessed 18 July, 2024). Despite the different experimental conditions compared to the present study, it appears therefore that the mixture of the two types of Gelucire® result in an overall higher CMC compared to the individual excipients. The presence of micelles able to solubilize lipophilic drug was further confirmed by the increased in KET crystalline solubility starting from a bit higher concentration value (750 μg/ml, Fig. 2). This small difference could be an indicator of the number of micelles needed to solubilize a detectable quantity of drug.

5.3. Gelucire impact on KET amorphous solubility

The solubility results suggested that Gel-mix impacts both KET equilibrium solubility in the water bulk phase as well as the LLPS onset, i.e., KET amorphous solubility. Fig. 9 provides a schematic overview of the three scenarios of KET supersaturated systems occurring with increasing Gelucire amounts.

Region I: At concentration ranging 1–50 μg/mL, Gel-mix is not able to improve drug solubilization, but affects the maximum achievable drug supersaturation, i.e., the drug amorphous solubility. In fact, KET amorphous solubility reduces further as more Gel-mix is added and reaches a minimum at 50 μg/mL. As a consequence, the amorphous-to-crystalline solubility ratio of KET decreased from a starting value of 2.8 in simple buffer to approximately 1.5 (Fig. 4b). It has been previously reported that the decreased amorphous solubility in presence of an additive depends on its interaction with the drug-rich droplets, resulting in a reduction in the thermodynamic activity of the drug in this phase as well as in the bulk aqueous phase (Ueda and Taylor, 2020). For example, HPMCAS decreased the LLPS onset from 40 μg/mL approximately 23 μg/mL as the polymer distributed to the drug-rich phase during LLPS due to strong intermolecular hydrogen bonding and hydrophobic interactions to the drug (Miao et al., 2019). Similar behavior was observed for ibuprofen, which amorphous solubility decreased when hypromellose (HPMC) or polyvinylpyrrolidone/vinyl acetate (PVP-VA) were present in solution (Ueda and Taylor, 2020).

Therefore, the observed decreased amorphous solubility of KET in presence of Gel-mix can be attributed to the interaction/mixing of Gelucire® components with the drug-rich droplets formed after LLPS. An interesting question would be which components of Gelucire® and

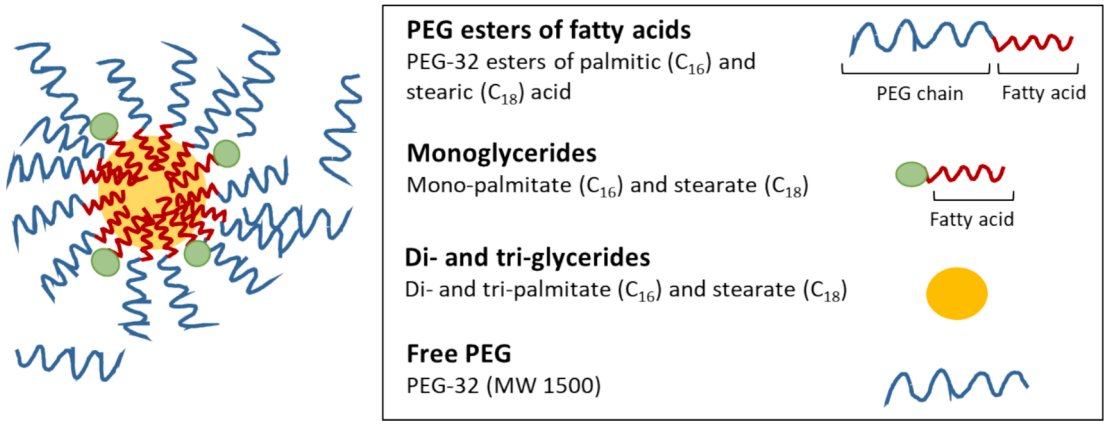

Fig. 8. Schematic representation of the structure of Gelucire micelles in aqueous solution.

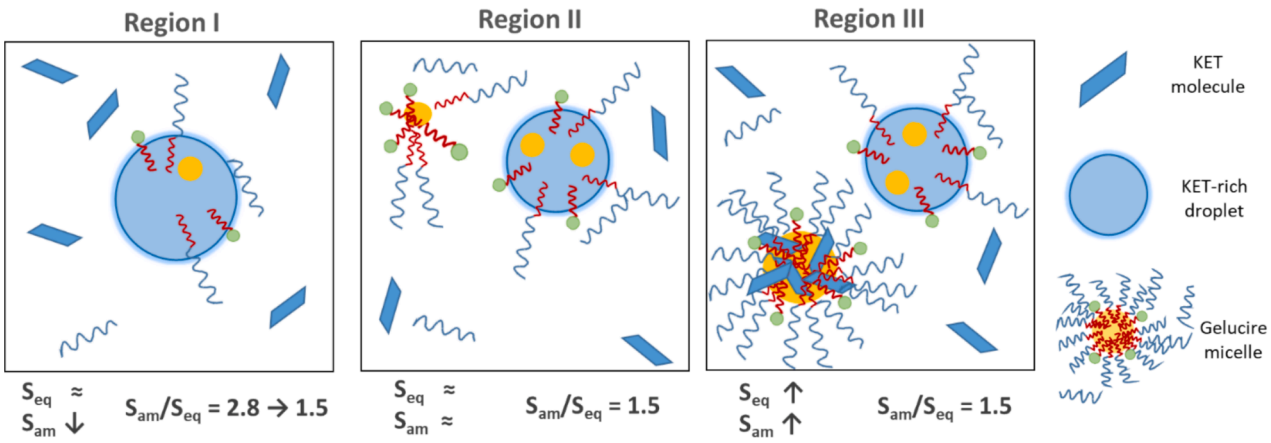

Fig. 9. Schematic illustration of Gelucire® effect on KET supersaturated solution: with increasing Gel-mix amounts, three situations characterized by different KET crystalline and amorphous solubilities occurred.

whether the monomeric or micellar form can actually interact with the KET nanodroplets. Since the effect of diminished LLPS onset was noted at Gel-mix concentration as low as 1 μg/mL (and no trace of micellar formation was observed at such concentration), it can be reasonably assumed that Gel-mix components as single molecules can interact with the drug-rich phase. As a general consideration, lipophilic molecules are more likely to mix with the hydrophobic drug-rich droplets in virtue of their similarity, whereas hydrophilic and ionized compounds tend to remain in the external aqueous phase. For example, the amorphous solubility of ritonavir was decreased when lopinavir, a lipophilic drug, was added to the supersaturated solution. Differently, in case of addition of an ionized drug (e.g. diclofenac), the drug amorphous solubility did not change (Bhesaniya et al., 2014). Among the various Gelucire® components, the lipophilicity of di- and triglyceride fraction might favor the mixing with the hydrophobic drug-rich phase. Moreover, an interaction between KET-rich droplets and the hydrophobic part of monoglycerides and PEG esters (presenting either hydrophobic and hydrophilic moieties) is possible. KET-rich droplets, in fact, have been observed to interact also with fairly hydrophilic polymers such as PVP or HPMC, resulting in a decrease of S_{am} comparable to that caused by Gel-mix at a concentration below CMC (100 μg/ml) (Fig. 4c).

Region II: Starting from Gel-mix concentration of 50 μg/mL, further increase in excipient amount did not further change drug amorphous solubility. Clearly, the partitioning of Gel-mix with the drug-phase is not proportional to the total amount of excipient added. In other words, the extent of mixing between Gelucire® and the drug-rich phase is favored up to a threshold, corresponding to 50 μg/mL, where the mixing is maximum. Gelucire® structures formed between 50 and 500 μg/ml are not able to accommodate KET molecules, or the solubilization is only transitory, since the S_{eq} was not significantly increased ($p > 0.001$, Fig. 2). The aggregates formed by self-association in the pre-micellar region might consist on transitory species formed by some Gel-mix components. In general, surfactant molecules below CMC may exist in the so-called premicellar state as dimers, tetramers and larger aggregates. These structures have been defined "pre-micellar aggregates" (Lombardo et al., 2019) and formed at the critical aggregation concentration (CAC). It has been previously observed that the CAC can be much smaller compared to the concentration at which stable micelles capable of solubilizing hydrophobic compounds are formed (Szutkowski et al., 2018).

However, Gelucire® pre-micellar structures can interact with the water-saturated drug-rich phase formed at LLPS causing the decrease of KET S_{am}. As a result, the amorphous-to-crystalline solubility ratio of KET remained constant at approximately 1.5 (Fig. 4b). The low amorphous-to-crystalline solubility ratio (as a result of the interaction of one excipient with the drug-rich phase at LLPS) is considered a negative aspect from the bioavailability perspective, since the maximum extent of supersaturation is decreased and consequently also the maximum rate of drug flux through the biological membranes. On the other hand, it is also possible that interface interactions between excipients and droplets surface may influence the drug-rich phase colloidal stability. This interaction regards hydrophilic additives that remains in the aqueous bulk phase but are adsorbed on the droplets surface either by ionic or nonionic interactions. This has been observed for the positively charged Eudragit E, which was adsorbed at the interface between ibuprofen-rich phase and the external aqueous phase (Ueda and Taylor, 2020). If this type of interaction takes place, the colloidal properties of the drug-rich droplets, including droplet size, Z-potential, polydispersity and stability, can be influenced. Thus, this phenomenon may comport advantages from the bioavailability perspective such as improved stability of the drug-rich droplets in terms of particle size resulting in lower tendency to coalesce and crystallize.

In case of Gel-mix, its hydrophilic components including free PEG chains, PEG portions of the esters and hydroxyl groups of the partial glycerides either as single entities or as hemimicelles may associate with the surface of the drug-rich phase, resulting a reduction of size and stabilization of the KET droplets (Fig. 5). Hemimicelles can be considered as clusters of surfactant molecules that behave as a surface-active layer able to interact with other molecules in the solution and may be formed at concentrations below the CMC (Erdinç et al., 2010). Being neutral molecules, the formation of ionic interaction is excluded but strong hydrogen bonds between the carboxylic group of KET and the hydroxyl groups of Gelucire have been reported (Bertoni et al., 2023).

Region III: In this region, Gelucire® micelles are able to improve drug solubilization by complexing/including drug molecules in their structures. KET exists in three different states: molecularly dissolved in the aqueous compartment, in the drug-rich phase and solubilized in the micelles. Accordingly, S_{eq} started to increase due to solubilization and S_{am} followed the same trend. For example, passing from Gel-mix amount of 500 to 1500 μg/mL (i.e., above its CMC), S_{eq} of KET increased from 175.8 ± 3.9 μg/mL to 305.1 ± 8.5 μg/mL, which is a factor of ~1.6 higher. In parallel, the LLPS onset was also found to increase to 496.9 ± 26.4 μg/mL, and this value is also a ~1.6 times higher than the S_{am} in 500 μg/mL Gel-mix (322.0 ± 9.4 μg/mL). These data showed that, above Gelucire CMC, KET S_{eq} increased and this led to a corresponding increase in the LLPS onset and therefore on S_{am}. This can be explained by considering that above CMC, further KET additions increased drug fraction solubilized in the micelles but not the molecular dissolved fraction. Since only the free drug in solution (and not the total concentration) corresponds to the solute thermodynamic activity, the fraction of drug solubilized in the micelles is irrelevant to the extent of supersaturation. Therefore, passing from region II to region III, where a

significant KET amount was solubilized by micellization (Fig. 2), concentration and activity of the drug were no longer equivalent. This led to a corresponding increase in the LLPS onset and therefore on the drug S_{am}, in accordance with previous observations indicating that the LLPS concentration is much higher when solubilizing additives are present (Raina et al., 2015). It should be kept in mind that, although the total drug concentration (and the LLPS onset) is higher in region III due to solubilization, the actual supersaturation extent observed in region III is identical to that in region II, and this explains why the amorphous-to crystalline solubility ratio is unchanged (Fig. 4b). This is further supported by the behaviour of PVP and HPMC, which, unable to form micelles, did not cause a similar increase in S_{eq} and S_{am} (Fig. 4c).

5.4. Gelucire impact on KET crystallization from supersaturated solutions

Results reported in Fig. 6a evidenced that Gel-mix concentration in the premicellar region (below 50 μg/ml) induces KET crystallization from supersaturates solution, when its concentration approaches the S_{am}. Similar observations were made for other surfactants such as SDS (Indulkar et al., 2020) and sodium dodecyl-(tertrapropy1)-benzenesulfonate (SDBS) (Michaels and Tausch, 1961) which accelerated the crystallization of small molecules compounds at concentrations lower that the CMC, where the surfactant could exist in monomers or hemimicelle structures. This effect can be explained by considering the interaction of surfactant monomers with the nuclei or crystal surfaces, leading to significant impact on crystal nucleation and growth (Canselier, 1993). Due to their amphiphilic properties, surfactants can adsorb at solid–liquid interfaces by interactions between their hydrophobic moieties and the growing crystals (Qazi et al., 2017). The interaction of Gelucire with the KET crystal surface also impact the size of the crystals formed, as shown in Fig. 6b.

Starting from Gel-mix concentration of 50 μg/ml, a switch in the crystallization kinetic of KET was observed. When Gel-mix components formed stable aggregates, the hydrocarbon chains of di- and triglyceride fraction are closed into micelles cores and therefore are no longer available to be absorbed on crystal nuclei, resulting in increased KET crystallization times. This holds true as long as the self-association of Gel-mix in micelles is preferred over the absorption of Gel-mix as monomers on KET crystal. The fact that KET crystallization time was significantly enhanced in solutions with Gel-mix amount above CMC (500 μg/ml) demonstrated that Gel-mix micelles, conversely to its individual monomers and to pure buffer, can act as effective crystallization inhibitors. This effect might depend on different mechanisms. It has been suggested that above CMC, surfactant can inhibit crystallization by a “passivation” of nucleation sites, meaning that the nucleation at the liquid/air interface is prevented by the presence of surfactants, thus leaving the bulk as only possible nucleation site. Since crystallization in bulk requires higher free energy, crystallization is inhibited (Qazi et al., 2017). The presence of micelles can slow down the mass transfer between bulk and crystal nuclei by a kinetic effect, thus reducing crystal growth (Canselier, 1993). Another possible explanation is the nucleation inside the lipophilic core of micelles (Canselier, 1993; Dvolaitzky et al., 1983). To further investigate this aspect, KET crystals were analysed by DSC (Fig. 7). The data suggest that in case of Gelucire below CMC, KET crystallized faster in the aqueous compartment, as a result of Gelucire individual components that can interact with crystal nuclei, resulting in imperfect crystals with decreased T_m. By contrast, Gelucire above CMC decrease crystallization kinetic by either slowing down crystal growth (as suggested by the nanosized crystals formed, Fig. 6b) or even the allowing the nucleation inside the lipophilic core of micelles (as suggested by the incorporation of Gel-mix components in the KET crystals, Fig. 9).

Finally, a consideration should be given to the effect of Gel-mix on drug crystallization from supersaturated solutions above the amorphous solubility, i.e., after LLPS. In pure buffer, KET-rich droplets tended to growth with increasing KET amounts (Fig. 5). This is consistent with previous reports, showing that an increase of oil concentration promotes destabilization of the oil droplets (Ueda and Taylor, 2020; Gupta et al., 2016). Accordingly, after LLPS, if more drug is added to the system, the free drug concentration does not increase, instead more disperse phase is formed (Raina et al., 2015). It should be kept in mind that the growth and coarsening of the drug-rich phase often precede the development of crystalline phases: LLPS can be considered a precursor to crystallization since in the drug-rich droplets the drug molecules are in close proximity to each other and might be easily subjected to nuclei formation (Jackson et al., 2016; Sun et al., 2016). Thus, the ability of an excipient to stabilize drug-rich droplets is considered a positive effect possibly delaying crystallization and prolonging the supersaturation duration.

Based on the droplet size analysis (Fig. 5), it appears that among the tested excipients, PVP proved to be ineffective at preventing the coarsening of drug-rich droplets at increasing KET amounts. HPMC showed a moderate inhibition effect on the coarsening of the KET-rich phase after formation while Gel-mix led to the highest colloidal stability of KET-nanodroplets after LLPS. The mechanisms at the basis of the improved colloidal stability may include reduced interfacial tension at the nanodroplets surface and reduction rate of Ostwald ripening, which is the main cause of physical destabilization of an emulsion when the droplets are sufficiently small (Tadros et al., 2004). These effects can be related to the earlier discussed interaction of Gel-mix components to the KET-rich droplets. The crystallization times of KET from supersaturated solution above S_{am} (Table 1) further support this result. The crystallization inhibition effect, starting from 50 μg/ml Gel-mix concentration, confirms the effectiveness of high HLB Gelucire excipients in preventing crystal nuclei formation as a result of the improved colloidal stability of the drug-rich phase.

6. Conclusion

This study showed that Gelucire® excipients with high HLB values might have a profound influence on LLPS and crystallization of a poorly water-soluble drug from supersaturated solutions. When present as monomers (below 50 μg/mL), components of Gel-mix interact with the drug-rich phase formed at LLPS decreasing the amorphous solubility and the amorphous-to-crystalline solubility ratio. Further, they accelerate KET crystallization from supersaturates solution. On the opposite, at concentration levels of 50–500 μg/mL, Gelucire® components starts to self-aggregate into micelles and concentrations exceeding 500 μg/mL improved drug solubilization by inclusion into micelles, resulting in a gradual increase of both crystalline and amorphous solubility (but with constant amorphous-to-crystalline solubility ratio). At the same time, Gelucire® micelles inhibit KET crystallization from the supersaturated state for over 6 h and impact the crystal morphology. Notably, drug crystallization from supersaturated solutions is inhibited also above LLPS, as Gel-mix is able to improve the colloidal stability of the drug-rich phase limiting the enlargement of the droplets and thus preventing crystal nuclei formation. Gelucire® excipients showed a strong crystallization inhibition effect, comparable to traditional amorphous polymers (HPMC and PVP), but with the distinctive trait of being dependent on the micellar behaviour. Concluding, the results reported in this paper bring new insights on the role of high HLB Gelucire® excipients in the phase behaviour of supersaturated solutions of poorly water-soluble drug, allowing a better understanding of the properties of these systems and supporting a more appropriate excipients choice for SDDS formulation.

CRediT authorship contribution statement

Serena Bertoni: Writing – original draft, Methodology, Investigation, Data curation, Conceptualization. **Beatrice Albertini:** Writing – review & editing, Supervision, Methodology. **Nadia Passerini:** Writing – review & editing, Supervision, Funding acquisition.

Declaration of competing interest

The authors declare that they have no known competing financial interests or personal relationships that could have appeared to influence the work reported in this paper.

Acknowledgments

This research did not receive any specific grant from funding agencies in the public, commercial, or not-for-profit sectors.

The authors acknowledge Gattefossè for the supply of Gelucire® 50/13 and Gelucire® 48/16.

Data availability

Data will be made available on request.

References

Albertini, B., Sabatino, M.D., Melegari, C., Passerini, N., 2015. Formulation of spray congealed microparticles with self-emulsifying ability for enhanced glibenclamide dissolution performance. J. Microencapsul. 32, 181–192. https://doi.org/10.3109/02652048.2014.985341.

Aldosari, B.N., Almurshedi, A.S., Alfagih, I.M., AlQuadeib, B.T., Altamimi, M.A., Imam, S.S., Hussain, A., Alqahtani, F., Elzayat, E., Alshehri, S., 2021. Formulation of Gelucire®-based solid dispersions of atorvastatin calcium: in vitro dissolution and in vivo bioavailability study. AAPS PharmSciTech 22, 161. https://doi.org/10.1208/s12249-021-02019-5.

Alhayali, A., Selo, M.A., Ehrhardt, C., Velaga, S., 2018. Investigation of supersaturation and in vitro permeation of the poorly water soluble drug ezetimibe. Eur. J. Pharm. Sci. 117, 147–153. https://doi.org/10.1016/j.ejps.2018.01.047.

Bertoni, S., Albertini, B., Ferraro, L., Beggiato, S., Dalpiaz, A., Passerini, N., 2019. Exploring the use of spray congealing to produce solid dispersions with enhanced indomethacin bioavailability: in vitro characterization and in vivo study. Eur. J. Pharm. Biopharm. 139, 132–141. https://doi.org/10.1016/j.ejpb.2019.03.020.

Bertoni, S., Albertini, B., Passerini, N., 2020. Different BCS class II drug-gelucire solid dispersions prepared by spray congealing: evaluation of solid state properties and in vitro performances. Pharmaceutics 12. https://doi.org/10.3390/pharmaceutics12060548.

Bertoni, S., Albertini, B., Passerini, N., 2023. Investigating the physicochemical properties of solid dispersions based on semicrystalline carriers: a case study with ketoprofen. Int. J. Pharm. 632, 122576. https://doi.org/10.1016/j.ijpharm.2022.122576.

Bhesaniya, K., Nandha, K., Baluja, S., 2014. Thermodynamics of fluconazole solubility in various solvents at different temperatures. J. Chem. Eng. Data 59, 649–652. https://doi.org/10.1021/je4010257.

Brouwers, J., Brewster, M.E., Augustijns, P., 2009. Supersaturating drug delivery systems: the answer to solubility-limited oral bioavailability? J. Pharm. Sci. 98, 2549–2572. https://doi.org/10.1002/jps.21650.

Canselier, J.P., 1993. The effects of surfactants on crystallization phenomena. J. Dispers. Sci. Technol. 14, 625–644. https://doi.org/10.1080/01932699308943435.

Chen, J., Ormes, J.D., Higgins, J.D., Taylor, L.S., 2015. Impact of surfactants on the crystallization of aqueous suspensions of celecoxib amorphous solid dispersion spray dried particles. Mol. Pharmaceutics 12, 533–541. https://doi.org/10.1021/mp5006245.

Dahan, A., Beig, A., Lindley, D., Miller, J.M., 2016. The solubility–permeability interplay and oral drug formulation design: two heads are better than one. Adv. Drug Deliv. Rev. 101, 99–107. https://doi.org/10.1016/j.addr.2016.04.018.

Dai, W.-G., Dong, L.C., Li, S., Deng, Z., 2008. Combination of Pluronic/Vitamin E TPGS as a potential inhibitor of drug precipitation. Int. J. Pharm. 355, 31–37. https://doi.org/10.1016/j.ijpharm.2007.12.015.

Daravath, B., 2021. Surface solid dispersion: a novel method for improving in-vitro dissolution and in-vivo pharmacokinetics of meclizine hydrochloride. Research Journal of Pharmacy and Technology 14, 685–693. https://doi.org/10.5958/0974-360X.2021.00121.9.

Dvolaitzky, M., Ober, R., Taupin, C., Anthore, R., Auvray, X., Petipas, C., Williams, C., 1983. Silver chloride microcrystals suspensions in microemulsion media. J. Dispers. Sci. Technol. 4, 29–45. https://doi.org/10.1080/01932698308943354.

Erdinç, N., Göktürk, S., Tunçay, M., 2010. A study on the adsorption characteristics of an amphiphilic phenothiazine drug on activated charcoal in the presence of surfactants. Colloids Surf. B Biointerfaces 75, 194–203. https://doi.org/10.1016/j.colsurfb.2009.08.031.

Gattefossè website. https://www.gattefosse.com/pharmaceuticals/product-finder/gelucire-4816 (accessed 18 July 2024).

Gattefossè website. https://www.gattefosse.com/pharmaceuticals/product-finder/gelucire-5013 (accessed 18 July 2024).

Goo, Y., Sa, C.-K., Choi, J., Kim, M., Kim, C., Kim, H., Choi, Y., 2021. Development of a solid supersaturable micelle of revaprazan for improved dissolution and oral bioavailability using box-behnken design. Int. J. Nanomed. 16, 1245–1259. https://doi.org/10.2147/IJN.S298450.

Gupta, A., Eral, H.B., Hatton, T.A., Doyle, P.S., 2016. Nanoemulsions: formation, properties and applications. Soft Matter 12, 2826–2841. https://doi.org/10.1039/C5SM02958A.

Ilevbare, G.A., Taylor, L.S., 2013. Liquid-liquid phase separation in highly supersaturated aqueous solutions of poorly water-soluble drugs: implications for solubility enhancing formulations. Cryst. Growth Des. 13, 1497–1509. https://doi.org/10.1021/cg301679h.

Indulkar, A., Gao, Y., Raina, S., Zhang, G., Taylor, L., 2020. Impact of monomeric vs. micellar surfactant and surfactant-polymer interactions on nucleation-induction times of atazanavir from supersaturated solutions. Cryst. Growth Des. 20, 62–72. https://doi.org/10.1021/acs.cgd.9b00482.

Jackson, M.J., Kestur, U.S., Hussain, M.A., Taylor, L.S., 2016. Characterization of supersaturated danazol solutions – impact of polymers on solution properties and phase transitions. Pharm. Res. 33, 1276–1288. https://doi.org/10.1007/s11095-016-1871-y.

Lombardo, D., Munaò, G., Calandra, P., Pasqua, L., Caccamo, M.T., 2019. Evidence of pre-micellar aggregates in aqueous solution of amphiphilic PDMS–PEO block copolymer. Phys. Chem. Chem. Phys. 21, 11983–11991. https://doi.org/10.1039/C9CP02195G.

Miao, L., Liang, Y., Pan, W., Gou, J., Yin, T., Zhang, Y., He, H., Tang, X., 2019. Effect of supersaturation on the oral bioavailability of paclitaxel/polymer amorphous solid dispersion. Drug Deliv. Transl. Res. 9, 344–356. https://doi.org/10.1007/s13346-018-0582-9.

Michaels, A.S., Tausch, F.W.Jr, 1961. Modification of growth rate and habit of adipic acid crystals with surfactants. J. Phys. Chem. 65, 1730–1737. https://doi.org/10.1021/j100827a014.

R. Miller, V. Fainerman, Surfactant Adsorption Layers at Liquid-Fluid Interfaces, in: 2001: pp. 383–421. 10.1016/B978-012513910-6/50013-X.

Mullin, J.W., Söhnel, O., 1977. Expressions of supersaturation in crystallization studies. Chem. Eng. Sci. 32, 683–686. https://doi.org/10.1016/0009-2509(77)80114-0.

Nguyen, H.T., Van Duong, T., Jaw-Tsai, S., Bruning-Barry, R., Pande, P., Taneja, R., Taylor, L.S., 2023. Fed- and fasted-state performance of pretomanid amorphous solid dispersions formulated with an enteric polymer. Mol. Pharmaceutics 20, 3170–3186. https://doi.org/10.1021/acs.molpharmaceut.3c00174.

Panigrahi, K.C., Patra, C.N., Jena, G.K., Ghose, D., Jena, J., Panda, S.K., Sahu, M., 2018. Gelucire: a versatile polymer for modified release drug delivery system. Future Journal of Pharmaceutical Sciences 4, 102–108. https://doi.org/10.1016/j.fjps.2017.11.001.

Perinelli, D.R., Cespi, M., Lorusso, N., Palmieri, G.F., Bonacucina, G., Blasi, P., 2020. Surfactant self-assembling and critical micelle concentration: one approach fits all? Langmuir 36, 5745–5753. https://doi.org/10.1021/acs.langmuir.0c00420.

Qazi, M.J., Liefferink, R.W., Schlegel, S.J., Backus, E.H.G., Bonn, D., Shahidzadeh, N., 2017. Influence of surfactants on sodium chloride crystallization in confinement. Langmuir 33, 4260–4268. https://doi.org/10.1021/acs.langmuir.7b00244.

Qi, S., Marchaud, D., Craig, D.Q.M., 2010. An investigation into the mechanism of dissolution rate enhancement of poorly water-soluble drugs from spray chilled gelucire 50/13 microspheres. J. Pharm. Sci. 99, 262–274. https://doi.org/10.1002/jps.21832.

Raina, S.A., Zhang, G.G.Z., Alonzo, D.E., Wu, J., Zhu, D., Catron, N.D., Gao, Y., Taylor, L.S., 2015. Impact of solubilizing additives on supersaturation and membrane transport of drugs. Pharm. Res. 32, 3350–3364. https://doi.org/10.1007/s11095-015-1712-4.

Raina, S.A., Alonzo, D.E., Zhang, G.G.Z., Gao, Y., Taylor, L.S., 2015. Using environment-sensitive fluorescent probes to characterize liquid-liquid phase separation in supersaturated solutions of poorly water soluble compounds. Pharm. Res. 32, 3660–3673. https://doi.org/10.1007/s11095-015-1725-z.

Reporting Experimental Data Dealing with Critical Micellization Concentrations (c.m.c's) of Aqueous Surfactant. Systems 51, 1979, 1083–1090. https://doi.org/10.1351/pac197951051083.

Sarabu, S., Kallakunta, V.R., Butreddy, A., Janga, K.Y., Ajjarapu, S., Bandari, S., Zhang, F., Murthy, S.N., Repka, M.A., 2021. A one-step twin-screw melt granulation with gelucire 48/16 and surface adsorbent to improve the solubility of poorly soluble drugs: effect of formulation variables on dissolution and stability. AAPS PharmSciTech 22, 79. https://doi.org/10.1208/s12249-021-01945-8.

Semjonova, A., Bērziņš, A., 2022. Surfactant provided control of crystallization polymorphic outcome and stabilization of metastable polymorphs of 2,6-dimethoxyphenylboronic acid. Crystals 12. https://doi.org/10.3390/cryst12121738.

Shin, D.J., Chae, B.R., Goo, Y.T., Yoon, H.Y., Kim, C.H., Sohn, S.I., Oh, D., Lee, A., Song, S.H., Choi, Y.W., 2019. Improved dissolution and oral bioavailability of valsartan using a solidified supersaturable self-microemulsifying drug delivery system containing Gelucire® 44/14. Pharmaceutics 11. https://doi.org/10.3390/pharmaceutics11020058.

Sun, D.D., Wen, H., Taylor, L.S., 2016. Non-sink dissolution conditions for predicting product quality and in vivo performance of supersaturating drug delivery systems. J. Pharm. Sci. 105, 2477–2488. https://doi.org/10.1016/j.xphs.2016.03.024.

Szutkowski, K., Kołodziejska, Ż., Pietralik, Z., Zhukov, I., Skrzypczak, A., Materna, K., Kozak, M., 2018. Clear distinction between CAC and CMC revealed by high-resolution NMR diffusometry for a series of bis-imidazolium gemini surfactants in aqueous solutions. RSC Adv. 8, 38470–38482. https://doi.org/10.1039/C8RA07081D.

Tadros, T., Izquierdo, P., Esquena, J., Solans, C., 2004. Formation and stability of nano-emulsions. Adv. Colloid Interface Sci. 108–109, 303–318. https://doi.org/10.1016/j.cis.2003.10.023.

Ueda, K., Taylor, L.S., 2020. Polymer type impacts amorphous solubility and drug-rich phase colloidal stability: a mechanistic study using nuclear magnetic resonance

spectroscopy. Mol. Pharmaceutics 17, 1352–1362. https://doi.org/10.1021/acs.molpharmaceut.0c00061.

Uttreja, P., Youssef, A.A., Karnik, I., Sanil, K., Narala, N., Wang, H., Elkanayati, R.M., Vemula, S.K., Repka, M.A., 2024. Formulation development of solid self-nanoemulsifying drug delivery systems of quetiapine fumarate via hot-melt extrusion technology: optimization using central composite design. Pharmaceutics 16. https://doi.org/10.3390/pharmaceutics16030324.

Vithani, K., Goyanes, A., Jannin, V., Basit, A.W., Gaisford, S., Boyd, B.J., 2019. A proof of concept for 3D printing of solid lipid-based formulations of poorly water-soluble drugs to control formulation dispersion kinetics. Pharm. Res. 36. https://doi.org/10.1007/s11095-019-2639-y.

Wang, Z., Lou, H., Dening, T.J., Hageman, M.J., 2023. Biorelevant dissolution method considerations for the appropriate evaluation of amorphous solid dispersions: are two stages Necessary? J. Pharm. Sci. 112, 1089–1107. https://doi.org/10.1016/j.xphs.2022.12.008.

Yazdanian, M., Briggs, K., Jankovsky, C., Hawi, A., 2004. The “High Solubility” definition of the current FDA guidance on biopharmaceutical classification system may be too strict for acidic drugs. Pharm. Res. 21, 293–299. https://doi.org/10.1023/B:PHAM.0000016242.48642.71.

Zoubari, G., Staufenbiel, S., Volz, P., Alexiev, U., Bodmeier, R., 2017. Effect of drug solubility and lipid carrier on drug release from lipid nanoparticles for dermal delivery. Eur. J. Pharm. Biopharm. 110, 39–46. https://doi.org/10.1016/j.ejpb.2016.10.021.